Conclusions

In wide ranges of the mixture ratios, fill pressures, and obturator mass, thermally choked combustion is initiated by the shock generated on the upstream surface of the obturator when the obturator reaches the combustible mixture in the ram-accelerator tube. This occurs as long as the shock generated on the obturator surface is strong enough to ignite the mixture. However, sustainability of the thermally choked combustion and the near-normal shock on the projectile strongly depends on the following two key factors: 1) the energy release rate in combustion process and 2) the separation speed between the obturator and projectile. If energy release in the combustion process is too strong or the obturator does not separate fast enough from the projectile, the shock overtakes the projectile. If energy release is too weak or the obturator separates too fast from the projectile, the shock falls off the projectile. The basic understanding of the initiation mechanism and the additional analyses based on the different simulations discussed in this study provide important guidelines on how to select the different parameters to achieve a sustained near-normal shock and projectile acceleration.

Acknowledgments

This work was supported by the Office of Naval Research through both the U.S. Naval Surface Warfare Center, Dahlgren Division, and the U.S. Naval Research Laboratory.

References

[1]Hertzberg, A., Bruckner, A. P., and Bogdanoff, D. W., "Ram Accelerator: A New Chemical Method for Accelerating Projectiles to Ultrahigh Velocities," *AIAA Journal*, Vol. 26, No. 2, 1988, pp. 195–203.

[2]Li, C., Kailasanath, K., and Oran, E. S., "Dynamics of Oblique Detonations in Ram Accelerators," *Shock Waves*, Vol. 5, No. 5, 1995, pp. 97–102.

[3]Li, C., Kailasanath, K., and Oran, E. S., "Detonation Structures on Ram-Accelerator Projectiles," AIAA Paper 94-0551, Jan. 1994.

[4]Bruckner, A. P., Knowlen, C., Hertzberg, A., and Bogdanoff, D. W., "Operational Characteristics of the Thermally Choked Ram Accelerator," *Journal of Propulsion and Power*, Vol. 7, No. 1, 1991, pp. 15–26.

[5]Li, C., Kailasanath, K., and Oran, E. S., "Analysis of Transient Flows in Thermally Choked Ram Accelerator," AIAA Paper 93-2187, June 1993.

[6]Kruczynski, D. L., and Liberatore, F., "Experimental Investigation of High Pressure/Performance Ram Accelerator Operation," AIAA Paper 96-2676, July 1996.

[7]Boris, J. P., and Book, D. L., "Solution of the Continuity Equations by the Method of Flux-Corrected Transport," *Methods of Computational Physics*, Vol. 16, No. 1, 1976, pp. 85–107.

[8]Oran, E. S., Boris, J. P., Young, T., Flanigan, M., Burk, T., and Picone, M., "Numerical Simulations of Detonations in Hydrogen-Air and Methane-Air Mixtures," *Proceedings of the 18th International Symposium on Combustion*, The Combustion Inst., Pittsburgh, PA, Vol. 18, 1981, pp. 1641–1649.

[9]Peterson, E. L., Davidson, D. F., and Hanson, R. K., "Reduced Kinetics Mechanisms for Ram Accelerator Combustion," AIAA Paper 97-2892, July 1997.

[10]Landsberg, A. M., Young, T. R., and Boris, J. P., "An Efficient, Parallel Method for Solving Flows in Complex Three-Dimensional Geometries," AIAA Paper 94-0413, Jan. 1994.

[11]Li, C., Kailasanath, K., and Oran, E. S., "Analysis of Stability of Projectiles in Thermally Choked Ram Accelerators," AIAA Paper 96-0344, Jan. 1996.

[12]Li, C., Kailasanath, K., and Oran, E. S., "Detonation Structures Behind Oblique Shocks," *Physics of Fluids*, Vol. 6, No. 4, 1994, pp. 1600–1605.

[13]Stewart, J. F., Knowlen, C., and Bruckner, A. P., "Effects of Launch Tube Gases on Starting of the Ram Accelerator," AIAA Paper 97-3175, July 1997.

[14]Li, C., Kailasanath, K., and Oran, E. S., "Effects of Boundary Layers on Oblique-Detonation Structures," AIAA Paper 93-0450, Jan. 1993.

Noise-Suppressing Nozzle Calculation with Turbulent Viscosity

S. Bosniakov,* V. Vlasenko,† S. Matyash,†
and N. Yatskevich†
TsAGI, 140160, Moscow Region, Russia

Nomenclature

NPR = nozzle pressure ratio, $p_{t,n}/p_a$
p_a = ambient pressure
$p_{t,j}$ = jet total pressure
$p_{t,n}$ = average total pressure at the nozzle entry
x_k, x, y, z = Cartesian coordinates, k = 1, 2, 3

Introduction

THE development of exhaust system for future supersonic transport aircraft is closely connected with jet noise reduction. One of the ways to solve this problem assumes the use of an ejector nozzle, where a noise suppression effect is partly achieved by mixing a high-speed jet with ambient air. Experimental investigation of thrust and acoustic characteristics of a noise-suppressing nozzle (NSN) is a rather difficult task; therefore, it's necessary to combine wind-tunnel tests with numerical simulations. First-stage calculations based on a three-dimensional Euler equation system (EUL) for inviscid compressible perfect gas are published.[1] This Note presents second-stage calculations that use a three-dimensional Favre-averaged Euler equation system describing turbulent flows of inviscid compressible perfect gas, i.e., only free turbulence is considered, boundary layers are not simulated. This equation system is closed using a ($q - \omega$) model of turbulence.[2] The effects of turbulence compressibility are described by a simple TRB approach.[3] A new version of the computational fluid dynamics (CFD) code has been prepared by Yatskevich. The objective of this publication is to compare results using the same geometry and grid, but different physical models of the flow. It allows one to evaluate the turbulence contribution to NSN integral characteristics.

Basic equations and the CFD method are described in Ref. 1. A mathematical model of the nozzle was created in accordance with the plots for the real experimental model manufacturing.[1] It consists of several parts: duct, lobes, ejector, central body, flaps, etc. The computational grid in the nozzle was constructed with the use of a multiblock approach. The total grid consists of 137 blocks (650,000 cells).[1] The size of the computational cells in the region of mixing is about 1/16 the distance between neighboring lobes. The outer boundaries of the computational domain are distanced from the NSN surface to remove the influence of boundary conditions on the flow inside the nozzle. This distance is equal to the characteristic length of the task, the full length of the NSN model (~0.5 m). The largest computational cells (near the outer boundaries) are approximately 65 times larger than the cells in the region of mixing.

Results of Calculations and Experiments

Calculations were made at different values of nozzle pressure ratio (NPR), and different Mach numbers, M_a, for the ambient flow. The most interesting case for comparison in this

Received Oct. 23, 1997; revision received June 9, 1998; accepted for publication June 19, 1998.

*Head of CFD Group, Propulsion Department, Central Aerohydrodynamic Institute, Zhukovsky-3.

†Senior Researcher, Central Aerohydrodynamic Institute, Zhukovsky-3.

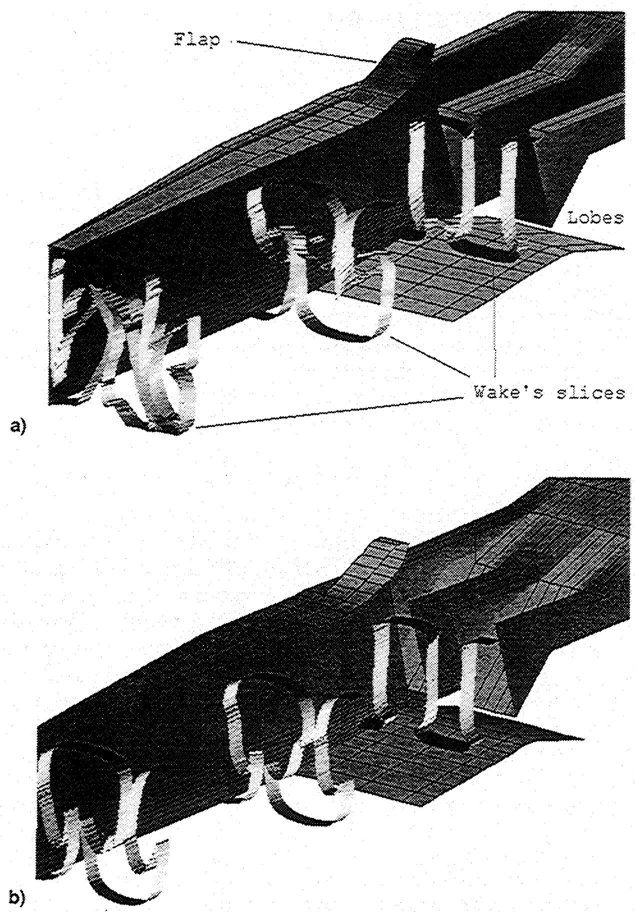

Fig. 1 Wake after the lobes in the mixer: a) Euler and b) turbulent viscosity.

Note is $M_a = 0$, when the Euler solution produces the maximum mistake because of the ejection, which is impossible to take into account.[1]

Another subject of great interest is the flow after the lobes. It's a well-known fact that the flow in the mixer after the lobes is characterized by numerous vortices that provide the mixing process. The CFD is shown in Fig. 1. Figure 1 contains two parts: Fig. 1a was prepared using the Euler equation system[1] (EUL), Fig. 1b is the result of calculations with turbulent viscosity taking TRB into account. It's easy to conclude that viscosity provides a smoother solution for the vortex sheet shape. Let's consider Fig. 2, where EUL results are combined with TRB and experimental ones.[1] The TRB of the vortex sheet slices are slightly closer to experimental data than that of the EUL. The wake cross section at the exit of the mixer is shown in Fig. 3. The EUL solution is compared with TRB. It is subscribed that the wake "surface" isn't smooth and that it contains some picks that create their own picture of interaction.[1] It is concluded that picks are the result of instability that is the feature of the Euler-obtained wake, and it is very similar to the Kelvin–Helmholtz phenomenon. Turbulent viscosity smooths the mixing layer in the CFD solution and diminishes the intensity of the previous picks. The results corresponds to the physical understanding of the phenomenon. On the basis of a time-averaged equation system, it is impossible to model the instability of the mixing layer because of the turbulent pulses generating inside this layer. Thus, the solution of the equations with viscosity must be smoother than the same solution in the inviscid case. The comparison in Fig. 3 confirms this idea.

Another important subject is the comparison of pressure measured in the experiment and that obtained by CFD. In Fig. 4, the total pressure distribution at the exit of mixer is dem-

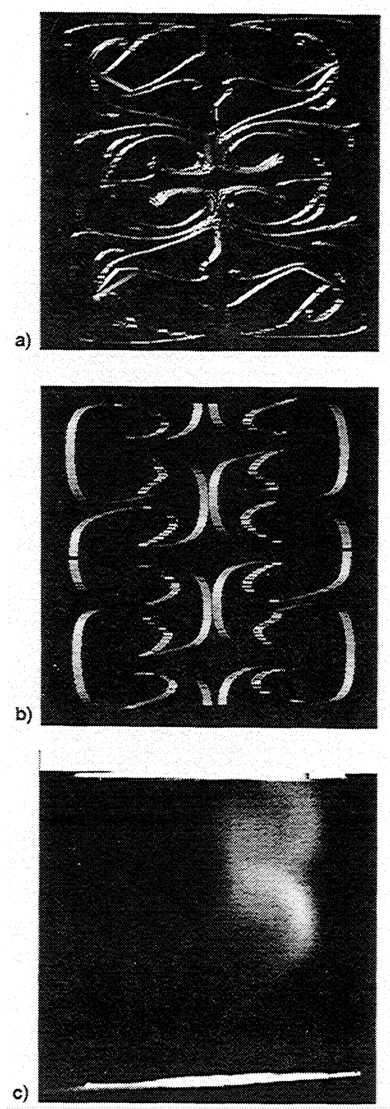

Fig. 2 Comparison of CFD and experimental data at the exit section: a) Euler, b) turbulent viscosity, and c) smoke screen.

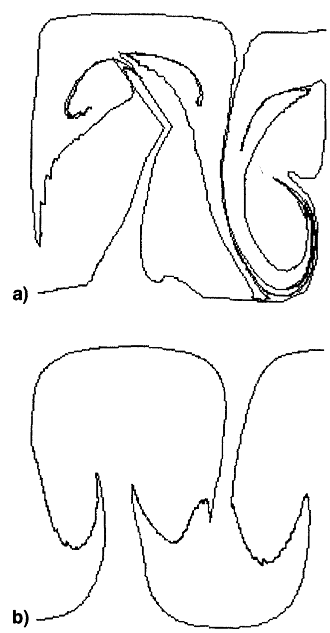

Fig. 3 Cross section of the wake slice: a) Euler and b) turbulent viscosity.

Table 1 Comparison of static pressure obtained by pressure dots, PSP methods, and CFD

	Numbers of pressure dots					
	1	2	3	4	5	6
EUL	0.909	0.929	0.867	0.907	1.012	0.977
TRB	0.947	0.833	0.747	0.715	0.967	1.034
Taps	0.965	0.892	0.708	0.723	0.945	1.008
PSP	——	——	0.72	0.774	0.943	1.015

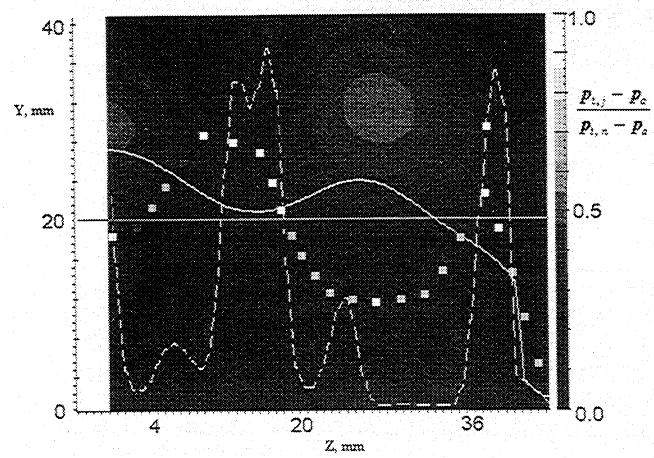

Fig. 4 Total pressure distribution at the exit section of ejector: ---, Euler; ——, turbulent viscosity; □, experiment.

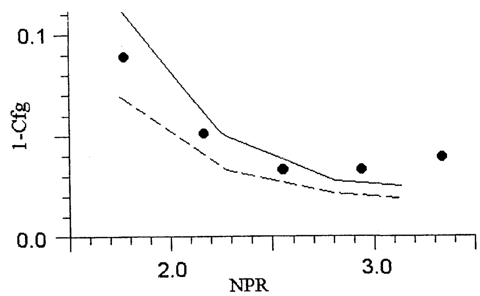

Fig. 5 Nozzle thrust losses: ---, Euler; ——, turbulent viscosity; ●, experiment.

onstrated, and the function of nondimensional total pressure $(p_{t,j} - p_a)/(p_{t,n} - p_a)$ is used. TRB data are compared with those of EUL and are depicted as having a black–white tone distribution. The chart in Fig. 4 shows the values of nondimensional total pressure along the white line in the middle of the figure. The solid line corresponds to the TRB data, the dashed line to the EUL ones, and the square markers are the experiment. It is obvious that the TRB data are in a poor qualitative agreement with the experiment. Turbulence viscosity in this case is too large to provide a good description of the mixture process after the lobes. This problem is the subject for future turbulence model investigations.

Comparison of the static pressure distribution along nozzle's side wall is shown in Table 1 for NPR = 2.75 (the averaged Mach number at the exit of the mixer is about 0.8). Experimental pressure distribution is obtained by the pressure taps with numbers 1–6[1] and by using pressure sensitive paints (PSP) technology. TRB data are much closer to the experiment (~5%) than those of EUL (up to 25%). Ejection caused by turbulent viscosity provides an additional rarefaction in the mixing area (dots 2 ÷ 4).

In Fig. 5, the TRB (solid line) and the EUL (dashed line) data for the thrust loss coefficient are compared with the experimental ones (●). When turbulence viscosity is taken into account, the computational curve is shifted and comes closer to experimental points. This indicates that ejection works. An extremely large shift shows that turbulence viscosity is too large and will result in additional thrust loss.

Conclusions

Results of calculations using a Favre-averaged Euler equation system closed by the $(q - \omega)$ model of turbulence show that 1) the main features of the flow in the nozzle mixer predicted earlier are confirmed, 2) the wake surface obtained in the TRB case is smoother than that in the EUL, 3) taking ejection into account improves the distribution of the static pressure on the wall, and 4) a detailed description of the total pressure distribution requires that the turbulent model be corrected.

Acknowledgments

This investigation was supported by the International Science and Technology Center in Moscow. Many thanks to S. Mikhailov who prepared the postprocessor's graphics and to M. Engulatova who worked with this article.

References

[1]Bosniakov, S., Fonov, S., Jitenev, V., Shenkin, A., Vlasenko, V., and Yatskevich, N., "Method for Noise Suppressing Nozzle Calculation and First Results of Its Implementation," *Journal of Propulsion and Power*, Vol. 14, No. 1, 1998, pp. 101–109.

[2]Coakley, T. J., "Turbulence Modeling Methods for the Compressible Navier-Stokes Equations," AIAA Paper 83-1693, July 1983.

[3]Dash, S., Weilersteen, G., and Vaglio-Laurin, R., "Compressibility Effects in Free Turbulent Shear Flows," Air Force Office of Scientific Research, TR-75-1436, 1975.

Development of a Strutjet Cold-Flow Mixing Experiment

David M. Spetman,* Clark W. Hawk,† and Marlow D. Moser‡
University of Alabama in Huntsville, Huntsville, Alabama 35899

Introduction

ROCKET-based combined cycle (RBCC) concepts attempt to improve the performance of launch vehicles at all points in the launch trajectory and make highly reusable launch vehicles a reality. The strutjet RBCC concept consists of a variable geometry duct with vertical struts inside that function in ducted rocket, ramjet, scramjet, and pure rocket modes.[1] These struts have rocket and turbine exhaust nozzles imbedded within them. The rocket flows induce an ejector effect with the ambient air at subsonic flight velocities. In ramjet and scramjet modes, the fuel-rich nozzle flows react with the ambient air, producing an afterburner effect. As shown in Fig. 1, the four primary rocket flows exit at the end of the strut with three turbine exhaust nozzles in between them. The strutjet is designed to mix the fuel-rich flows (rocket and turbine exhaust

Received Sept. 8, 1997; revision received June 27, 1998; accepted for publication July 6, 1998.

*Von Braun Propulsion Fellow, Propulsion Research Center, Department of Mechanical and Aerospace Engineering. Student Member AIAA.

†Director, Propulsion Research Center, also Professor, Department of Mechanical and Aerospace Engineering. Fellow AIAA.

‡Assistant Research Professor, Propulsion Research Center, Department of Mechanical and Aerospace Engineering. Member AIAA.